Pergamon
www.elsevier.com/locate/asr

Adv. Space Res. Vol. 29, No. 11, pp. 1673–1683, 2002

Printed in Great Britain
0273-1177/02 $22.00 + 0.00
PII: S0273-1177(02)00100-X

TROPOSPHERIC NO_2 FROM GOME MEASUREMENTS

A. Richter and J. P. Burrows [1]

[1] *Institute of Environmental Physics, University of Bremen, Kufsteinerstr. 1, 28359 Bremen, Germany*

ABSTRACT

Measurements from the Global Ozone Monitoring Experiment (GOME) have been analysed for tropospheric NO_2 using the Differential Optical Absorption method. The retrieval technique is described and a detailed error analysis is given. A case study of tropospheric NO_2 above Africa in fall 1997 is presented, showing the influence of both biomass burning and lightning. Comparison of clear and cloudy pixels reveals, that substantial amounts of NO_2 are present in the free troposphere over the African continent and in the outflow regions over the Southern Atlantic and the Indian Ocean. This has important implications for the formation of the tropospheric ozone maxima observed in these areas.

INTRODUCTION

The Nitrogen Dioxide radical is one of the key species in both stratospheric and tropospheric chemistry. In the stratosphere, it is involved in ozone destruction and the conversion of active halogen oxides into less active reservoirs. In the troposphere, it is one of the most important ozone precursors and locally also contributes to radiative forcing. The main tropospheric sources of NO_x are soil emissions, industrial burning processes, biomass burning and lightning, adding up to an estimated total of 38 TgN per year (*Lamarque et al.* [1996]. While the main sources and source regions of NO_x are known, large uncertainties remain on the individual source strengths and their latitudinal and seasonal variation. With the new generation of nadir viewing UV/vis satellite instruments measuring at moderate spectral resolution such as GOME, measurements of tropospheric NO_2 from space have become possible, and a clearer picture of the global NO_2 concentration is evolving. Currently, these measurements are still of limited accuracy, but ongoing developments in both the satellite instruments (SCIAMACHY, OMI, GEOSCIA) and the retrieval techniques will improve the accuracy of the satellite data to a point where they can not only be used in a qualitative, but also in a quantitative sense.

INSTRUMENT

The GOME (*Burrows et al.* [1999a]) is a grating pseudo double monochromator covering the spectral range of 240 to 790 nm at a spectral resolution of 0.2 – 0.4 nm. GOME observes light scattered back from the atmosphere and reflected from the ground in near a nadir viewing geometry. The ground pixel size is 320 km across track and 40 km along track for the three forward scans and 960×40 km^2 for the back scan. Global coverage is achieved within three days at the equator and within one day at 65°latitude. An extraterrestrial solar spectrum is measured via a diffusor plate once per day. The GOME instrument was launched on the European ERS-2 satellite in April 1995 and has been operational since July of that year. The ERS-2 satellite is in a sun-synchronous polar orbit with an equator crossing time of 10:30 local time. Consequently, GOME measurements over low and middle latitudes are always taken in the late morning (local time).

The main target of GOME is the determination of the global stratospheric ozone field. However, the broad spectral coverage and the relatively good spectral resolution also allows for the retrieval of a number of other trace gases that have structured absorptions in the UV and visible wavelength range. Under clear sky conditions, visible and near UV radiation reaches the surface, and provides GOME with a unique sensitivity towards tropospheric absorbers. In particular, GOME measurements have been used to study tropospheric SO_2 (*Eisinger and Burrows* [1998]), BrO (*Wagner and Platt* [1998], *Richter et al.* [1998]), HCHO (*Ladstätter-Weißenmayer et al.* [1999]; *Thomas et al.* [1998]; *Chance et al.* [2001]) and NO_2 (*Leue et al.* [2001]; *Velders et al.* [2001]).

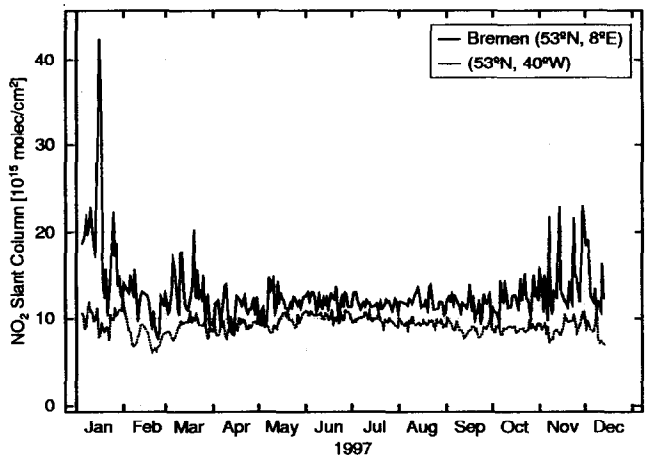

Fig. 1. Daily averages of GOME NO_2 slant columns for a 500 km area around Bremen and the corresponding latitude over the Atlantic Ocean. The seasonal variation in the NO_2 vertical column is compensated by the change in solar zenith angle for the GOME overpass at 53° North.

DATA ANALYSIS

In this study, tropospheric NO_2 columns are derived from GOME measurements in a series of steps described in the next paragraphs. Briefly, the NO_2 absorption in a single earth-shine spectrum is derived using the Differential Optical Absorption Spectroscopy (DOAS) technique. The stratospheric contribution to this absorption is estimated using a measurement taken at the same latitude over the Pacific, assuming that tropospheric NO_2 is negligible in this region. By subtracting the stratospheric column from the total column, a tropospheric slant column is derived that can be converted to a vertical tropospheric column using an appropriate airmass factor. The airmass factors is defined as the ratio of the observed slant column to the vertical column and is calculated with a radiative transfer model using a model atmosphere. To minimise the bias introduced by clouds shielding the troposphere from view, only measurements with a cloud cover below a certain threshold are included in the analysis.

NO_2 Slant Column Fit

Uncalibrated GOME earth-shine and solar spectra have been used to derive NO_2 slant columns with the DOAS algorithm developed for ground-based zenith-sky measurements (*Richter* [1997]). The wavelength interval 425–450 nm is used for the fit as the differential NO_2 absorption is largest and interference by other species is small. In addition to the NO_2 cross-section (*Burrows et al.* [1999b], ozone (*Burrows et al.* [1998]), O_4 (*Greenblatt et al.* [1990]), H_2O (*Rothman et al.* [1992]), a synthetic Ring spectrum (*Vountas et al.* [1998]), an undersampling correction (*Chance* [1998]) and an empirical calibration function are included in the fit. The calibration function is based on the polarisation dependency of the instrument measured before launch and was adjusted by hand to fit the observed residuals as closely as possible. This empirical adjustment is necessary as the instrument characteristics changed over time. In contrast to ground-based DOAS measurements, the GOME instrument takes direct measurements of the solar irradiance once per day, providing an absorption free background spectrum for the analysis. In principle, the daily solar spectra could be used as a background spectra to minimise the effects of instrumental drift. However, during one year slight changes in the incident angle of the solar radiation on the diffusor used for the solar measurements introduce systematic residuals that interfere with the NO_2 retrieval. Therefore, the extraterrestrial solar spectrum taken by GOME on February 28, 1997 is used as a background spectrum for all fits. This solar spectrum has been selected to give smallest residuals for the year 1997 and has been used throughout the analysis for consistency reasons. To optimise the spatial resolution, only the three forward scans are included in the analysis, thereby restricting the solar zenith angle range to values below 86°.

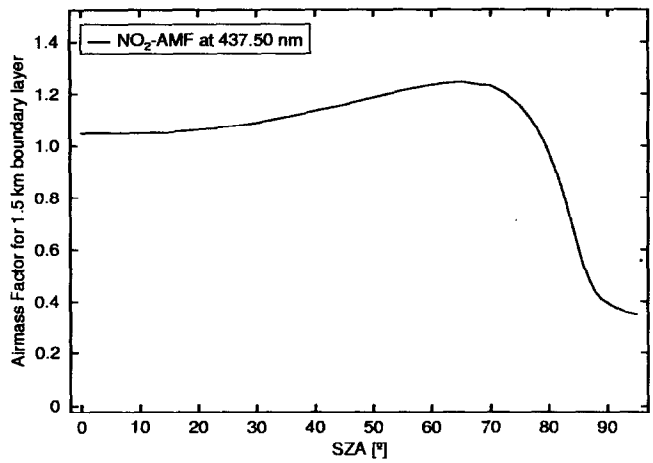

Fig. 2. Satellite airmass factor for a NO_2 layer in the lowermost 1.5 km, clear sky, surface albedo 0.05, maritime aerosols, and a wavelength of 437.5 nm.

Determination of the Stratospheric Background

In this study, the contribution of the stratospheric NO_2 to the measured slant column is estimated using two basic assumptions: longitudinal homogeneity of the stratospheric NO_2 layer and negligible tropospheric NO_2 over the Pacific between 180° and 190° longitude. As NO_2 in the stratosphere is mainly determined by day length (photolysis of the reservoirs) and only to a lesser degree by ozone concentrations and temperature, the first assumption is reasonable at low and middle latitudes. Longitudinal variations can clearly not be neglected close to the Polar Vortex or during major changes in stratospheric dynamics, introducing some artifacts at high latitudes in winter and spring. The use of the Pacific region as a clean air reference is justified by the results of both air-borne campaigns (see *Schultz et al.* [1999] and references therein) and the GOME measurements themselves, showing very little or no signature of anthropogenic or lightning produced NO_x.

As an example, GOME NO_2 slant columns are shown in Figure 1 for a 500 km area around Bremen (53°N, 8°E) and the corresponding latitude in a reference sector over the Atlantic for 1997.. For the slant column, the strong seasonal variation of the stratospheric NO_2 is compensated by the seasonal change in solar zenith angle at the time of the GOME overpass at this latitude. Comparing the two curves, both a general offset and large short-term pollution events, in particular in autumn, winter, and spring are evident. This result is typical for industrialised regions in the Northern hemisphere.

In the actual analysis, three days of GOME data are binned on a 0.25°×0.25°grid. As a result of the sun-synchronous polar orbit of ERS-2, fixed latitudes are always sampled at the same local time, implying the same solar zenith angle along a latitude band during a three day measurement cycle. It therefore is possible to subtract the stratospheric column as derived as the average over the longitude band in the Pacific sector without applying an airmass factor. The resulting values are the slant tropospheric columns.

Tropospheric Airmass Factor

The sensitivity of GOME measurements towards absorptions in the boundary layer depends on a number of parameters, including solar zenith angle, wavelength, cloud cover, absorber profile, aerosol loading and surface albedo. In this study, airmass factors have been calculated with the radiative transfer model GOMETRAN (*Rozanov et al.* [1997]) assuming clear sky conditions, a maritime aerosol, a surface albedo of 0.05 and a constant mixing ratio of NO_2 in the lowermost 1.5 km of the atmosphere. The resulting airmass factors for 437.5 nm are shown in Figure 2. Below 80° SZA, the airmass factor is nearly constant at a value of approximately 1. For larger SZA, the sensitivity towards the troposphere quickly decreases. This is in contrast to the stratospheric AMF that increases with increasing SZA and is largest at twilight (*Solomon et al.* [1987]).

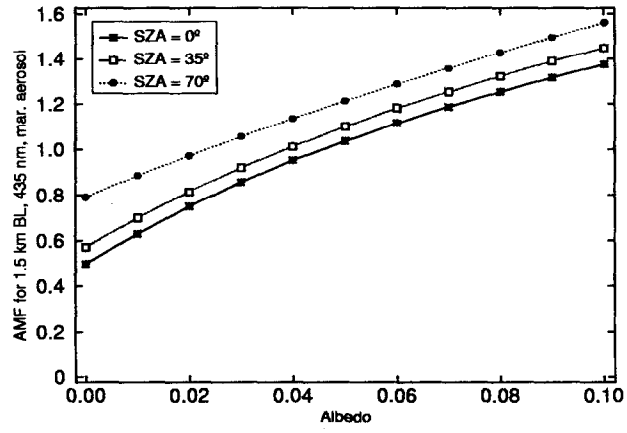

Fig. 3. Dependence of satellite airmass factor on the surface albedo. Except for the albedo, the scenario is identical to the one used for Figure 2.

One important input for the tropospheric AMF is surface albedo. As shown in Figure 3, the AMF for an absorber located in the boundary layer increases strongly with increasing surface albedo as the fraction of photons reflected back to the satellite instrument depends mainly on the absorption on the ground. To determine the appropriate surface albedo for the radiative transfer calculations, calibrated GOME radiances have been analysed in the wavelength window of the NO_2 fit. By scanning several months of data and saving the minimum value encountered in each 0.25×0.25 grid point, an approximation of the earth reflectance under cloud free conditions could be derived. From these reflectance values, the atmospheric contribution has been subtracted as computed with GOMETRAN for a Rayleigh atmosphere and an albedo of 0, resulting in an estimate of the surface albedo. In Figure 4, the resulting GOME surface albedo map is shown for all April measurements of 1997 - 2000. As can be seen, the albedo of land surfaces is low (smaller than 0.05 with the exception of deserts). The albedo of water is somewhat larger and depends on the viewing geometry relative to the sun, but generally is also in the range of 0.02 to 0.06. These results are in excellent agreement with a similar study using TOMS data at 380 nm (*Herman and Celarier* [1997]) and the wavelength dependent albedo measurements of *Feister and Grewe* [1995], justifying the assumption of an albedo of 0.05 as used in the airmass factor calculations. For a more detailed treatment of surface albedo, Mie-scattering on aerosols has also to be taken into account, but such an analysis is out of the scope of this paper.

Clouds

Space borne measurements in the UV-visible wavelength range are limited by clouds, that effectively act as reflecting surfaces. Therefore, if clouds are present, most of the boundary layer NO_2 is shielded from view and the satellite measurement is not representative for the integrated tropospheric column. To minimise this bias resulting from clouds, only measurements with a cloud cover fraction below 0.1 are included in the analysis. The cloud fraction used is taken from the operational GOME V2.7 lv2 data product (ICFA, *GOME* [1995]). Although this product is known to have problems in certain scenarios, it usually gives a fair estimate of the cloud conditions encountered during the GOME measurement (*Koelemeijer and Stammes* [1999]).

Comparison with previous GOME NO_2 studies

The tropospheric NO_2 analysis used in this work is very similar to that used in the study of *Leue et al.* [2001] and a second paper by (*Velders et al.* [2001]) that is based on the same data, but uses different assumptions for the airmass factors. As a result, the derived NO_2 slant columns are generally in good agreement. However, several important differences exist in the determination of the tropospheric columns, leading to significant differences in the derived tropospheric NO_2 vertical columns.

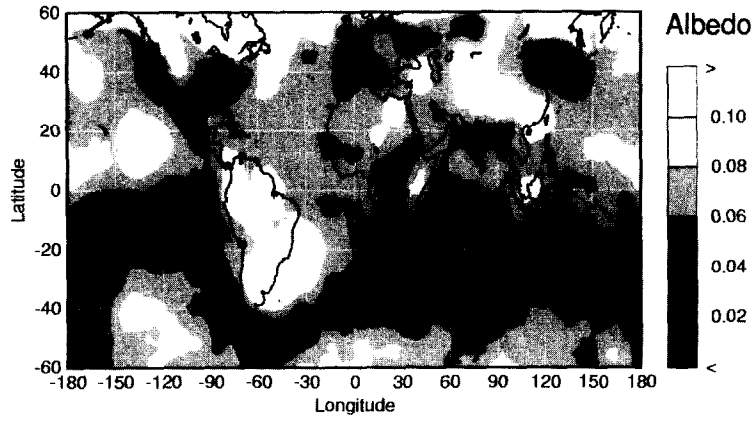

Fig. 4. Surface albedo at 437.5 nm as derived from GOME data. For each pixel, the minimum reflectivity from all GOME measurements taken in April 1997, 1998, 1999, and 2000 has been determined, and the atmospheric contribution as derived with GOMETRAN subtracted. In some areas, the derived albedo is contaminated by residual clouds (e.g. Indonesia), snow and ice (e.g. the Arctic) or the South Atlantic Anomaly. The GOME data have been smoothed for clarity.

Most importantly, instead of using the reference sector method described here, *Leue et al.* [2001] applied an image processing method to interpolate the stratospheric column from cloud covered pixels over the oceans at the same latitude. This reduces errors introduced by the longitudinal variation of stratospheric NO_2. However, the implicit assumption is, that tropospheric NO_2 above clouds is negligible everywhere over the oceans, which is in contradiction to the results shown in this paper (see Figure 8). As a result, NO_2 above the oceans and in central and southern Africa is underestimated under certain conditions.

Secondly, the surface albedo used in the airmass factor calculations of *Leue et al.* [2001] has been estimated using the GOME broad band Polarisation Measurement Devices (PMD) scaled to the values of *Li and Garand* [1994]. This procedure does not account for the strong decrease of surface albedo at shorter wavelengths (see Figure 4), overestimating the tropospheric airmass factor by as much as a factor of 2.5. As a result, the tropospheric NO_2 columns are underestimated by the same factor. This has been changed in the work of *Velders et al.* [2001], where the same airmass factors are used as in this paper.

The third difference is the treatment of clouds. In this study the analysis was restricted to pixels with an ICFA cloud fraction of less than 0.1, and no correction was applied to account for the residual cloud cover. *Leue et al.* [2001], however, used all data and applied a factor of 4 to the final tropospheric columns to correct for the cloud effect. On average, the resulting columns are larger by up to a factor of two than those derived in this study, and probably closer to the real tropospheric column (see error discussion in the next paragraph). However, the global application of a constant correction factor does not account for local differences in cloud statistics and potentially leads to large errors at locations with strong pollution and few clouds.

ERROR ANALYSIS

Several sources contribute to the overall error of the tropospheric NO_2 columns derived from GOME measurements: the uncertainty in the NO_2 fit, the uncertainty from the separation of troposphere and stratosphere, the uncertainty in the tropospheric light path and the uncertainty in cloud cover.

Uncertainty in the NO_2 Fit

The basic uncertainty of the NO_2 retrieval is given by the random error from the fit. For a typical GOME orbit, the random error of the slant column for an individual ground pixel is small, in the order of $2\text{-}4 \cdot 10^{14}$ molec/cm^2 (less than 5%) depending on the brightness of the scene. This value can further be reduced by averaging in space or time, making it negligible compared to other error sources. In addition to random errors, systematic errors can be introduced

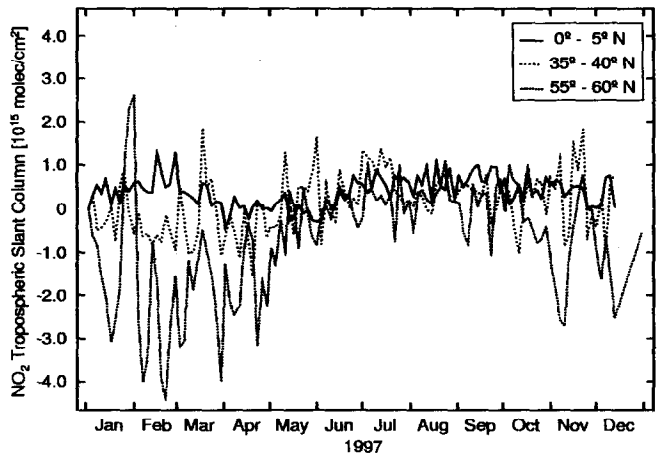

Fig. 5. Apparent tropospheric NO_2 slant column over the Atlantic (20°-30°W) in 1997. The negative values and large variability in winter and spring at high latitudes are a result of the low stratospheric NO_2 columns related to the very low stratospheric temperatures and are an artifact of the analysis.

by interference from other absorbers or instrument characteristics such as the change in solar background spectrum discussed above. These systematic errors are difficult to quantify, in particular as they tend to cancel out when using the reference sector method, where the difference of two GOME measurements taken under similar conditions is used. From the results of a large number of sensitivity tests we estimate, that a conservative limit for the systematic errors in the GOME NO_2 slant columns is $1 \cdot 10^{15}$ molec/cm^2.

An additional error is introduced by the temperature dependence of the NO_2 absorption cross-section. For the NO_2 fit, a cross-section appropriate for stratospheric temperatures (241 K) has been selected. However, the NO_2 in the boundary layer often is at much higher temperatures and therefore has smaller differential absorption structures than assumed. For a boundary layer temperature of 293 K, this effect will lead to a 20% underestimation of the tropospheric NO_2 column.

Uncertainty in the Separation of the Troposphere

For the separation of stratosphere and troposphere, the assumption of longitudinal homogeneity of the stratospheric NO_2 is made. While this assumption is reasonable at low latitudes, it breaks down in winter and spring when stratospheric NO_2 in polar regions is strongly reduced and zonal asymmetries in stratospheric temperatures lead to large zonal gradients. This is illustrated in Figure 5, where the apparent tropospheric NO_2 slant column over the Atlantic is plotted for different latitudes. As can be seen, the equatorial NO_2 is generally larger over the Atlantic than over the Pacific. This is to be expected as the influence of both pollution and biomass burning is smaller over the Pacific than over the Atlantic. However, at 55-60°N, very low values and a large variability are observed in winter and spring, in contrast to the small, but positive values expected. This behaviour is explained by the low stratospheric NO_2 columns resulting from the low temperatures that usually extend more to the south over the Atlantic than over the Pacific.

The numbers given in Figure 5 represent an extreme situation. In most cases, the region with low stratospheric NO_2 is restricted to Canada and the North Atlantic, and tropospheric measurements in both Europe and the US are not affected (see for example Figure 6, where values below $1 \cdot 10^{15}$ molec/cm^2 are rarely found). However, care should be taken when interpreting tropospheric NO_2 at high latitudes in spring and winter. In general, the error in the determination of the stratospheric contribution to the slant column can be estimated to be less than $1 \cdot 10^{15}$ molec/cm^2 in most cases.

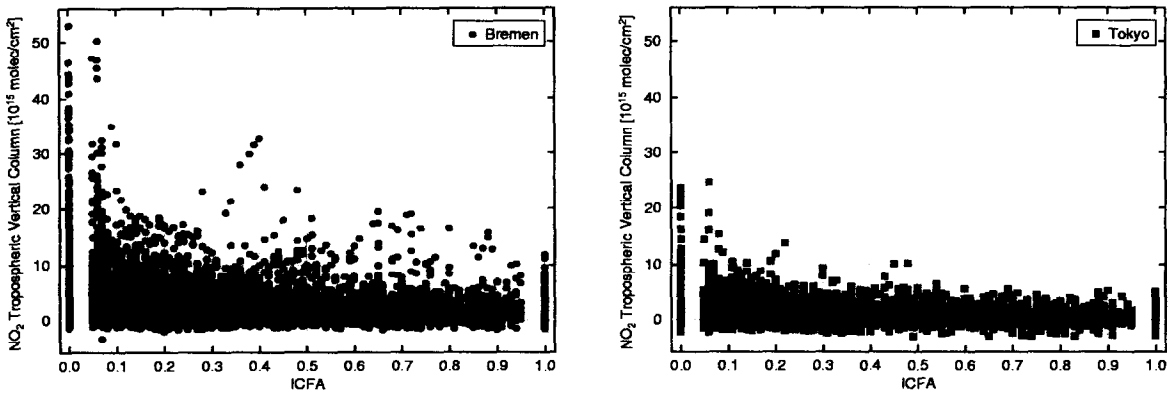

Fig. 6. Tropospheric NO_2 vertical columns as a function of the cloud fraction ICFA from the operational GOME product. In general, the largest tropospheric columns are observed for very low cloud cover. However, enhanced NO_2 is also observed at large cloud fraction, indicating substantial NO_2 above the clouds.

Uncertainty in the Tropospheric Light Path and Cloud Effects

By far the largest uncertainty in the tropospheric NO_2 results from the uncertainty in the tropospheric light path. From the albedo dependence alone, an error of up to 50% can be introduced for typical variations of surface albedo and even more for measurements over ice or snow if no correction is applied. The assumed value of 0.05 is on the high side for most scenarios and will in general lead to an underestimation of the tropospheric NO_2. The presence of absorbing aerosols will further reduce the sensitivity of GOME measurements to the lowermost troposphere as will reflecting aerosols situated over the bulk of the NO_2. If on the other hand a reflecting aerosol layer is situated below the NO_2, then the airmass factor will be increased and the NO_2 column be overestimated. In general, there will be a positive correlation between high NO_2 and large aerosol loading both in industrialised and biomass burning regions, decreasing the sensitivity of GOME towards the boundary layer in the main NO_2 source regions. Analysis of the airmass factors calculated for a range of reasonable assumptions leads to the conclusion, that for a NO_2 layer in the lowermost troposphere, the airmass factors for clear sky conditions can vary by as much as a factor of two.

Even larger uncertainties are introduced by residual clouds in the ground pixels. As a result of the large ground pixel size, most GOME measurements are contaminated by clouds, even if only those data with ICFA values smaller than 0.1 are used. In general, the NO_2 columns increase with decreasing cloud cover as shown in Figure 6 for two polluted sites. This is in agreement with the assumption, that most NO_2 resides below the clouds and is effectively shielded from view if clouds are present. However, elevated NO_2 levels are observed even for large cloud cover at both locations but in particular above Bremen. The most probable explanation is, that some NO_2 is present above the clouds, and that this effect is more important over Europe.

For the NO_2 above the cloud, the airmass factor adopted in this study is not appropriate, as clouds increase the effective albedo and thereby the sensitivity towards the troposphere. Thus, clouds will lead to an underestimation of NO_2 in the lowermost troposphere and at the same time to an overestimation of NO_2 above cloud top height.

The error introduced by the residual clouds in the used ground-pixels can be estimated by calculating the apparent NO_2 column as a function of cloud cover:

$$SC^{meas} = fSC^{cloudy}\frac{I^{cloudy}}{I^{total}} + (1-f)SC^{clear}\frac{I^{clear}}{I^{total}} \tag{1}$$

where f is the cloud fraction, SC the slant column calculated for a clear and a cloudy pixel, respectively, and I the intensity. While this equation assumes reflecting clouds and uses the intensity weighting approximation and therefore is not strictly valid, it should give a good approximation of the effect. In Figure 7, the results are shown for a SZA of 40°, 437.5nm, a surface albedo of 0.05, a cloud top height of 2 km and no NO_2 above the cloud. Assuming that the ICFA cloud fraction is correct, the tropospheric NO_2 column will be underestimated by up to 40% and much less on

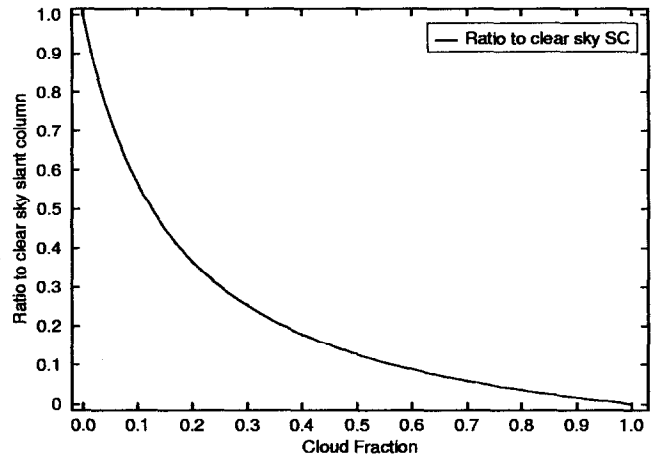

Fig. 7. Dependence of the apparent tropospheric NO_2 column on cloud cover. For this plot, a SZA of 40°, a cloud top height of 2 km and a surface albedo of 0.05 has been assumed, and the intensity weighting approximation been used.

average by using all data with a cloud cover of less than 0.1.

In addition to shielding the boundary layer from view, clouds can also increase the absorption if some NO_2 is present in the cloud and the light path is enhanced by multiple scattering. However, this effect is much smaller for satellite than for ground-based zenith-sky measurements (*Kurosu et al.* [1997]).

In summary, the accuracy of the tropospheric NO_2 columns derived from GOME measurements is limited by the uncertainties in tropospheric light path and clouds. Most error sources lead to a systematic underestimation of the tropospheric NO_2. Therefore, the GOME NO_2 columns for the troposphere derived in this study may be low by up to a factor of 2.

RESULTS

The algorithm described in the previous sections has been applied to GOME data covering the period January 1997 to May 2000. Here, we present a case study of tropospheric NO_2 above Africa, highlighting the detection of biomass burning and lightning sources of NO_2 and the effects of convection and horizontal transport of NO_2.

Lightning and Biomass Burning in Africa, Fall 1997

In the last years, the role of anthropogenic emissions on the global tropospheric ozone budget has been the focus of intense scientific research. In particular in the tropical regions, biomass burning seems to play an important role in the tropospheric ozone formation. In addition to direct production in the regions of the fires, the emission of ozone precursors from the fires and subsequent transport to remote regions including the Southern Atlantic has been recognised to be an important process. One of the most important ozone precursors is NO_x which is produced by industrial processes, biomass burning and lightning. Some evidence for the role of NO_x emissions from both fires and lightning has been found in airborne measurements over Southern Africa and the Atlantic (see e.g. *Thompson et al.* [1996]), but these measurements necessarily remain restricted in time and location. Tropospheric NO_2 columns from GOME can help to get a more concise picture of the temporal and spatial distribution of NO_2.

In Figure 8, two different evaluations of GOME NO_2 are shown for fall (September - November) 1997 over the African continent: one using only clear sky pixels (ICFA < 0.1) and one using only cloudy pixels (ICFA > 0.3). In the clear sky data, NO_2 emissions from biomass burning in southern Africa and Brazil (see ATSR fire counts, *European Space Agency ESA/ESRIN via Galileo Galilei CP 64 00044 Frascati Italy* [2000]) can clearly be identified. Anthropogenic emissions over Europe, the Arabian peninsula and South Africa are also visible in the measurements. In addition, there is a background of elevated NO_2 over parts of Africa, where little biomass burning takes place in this season. These regions coincide with the area of intense thunderstorm activity as seen in the OTD (*Christian*

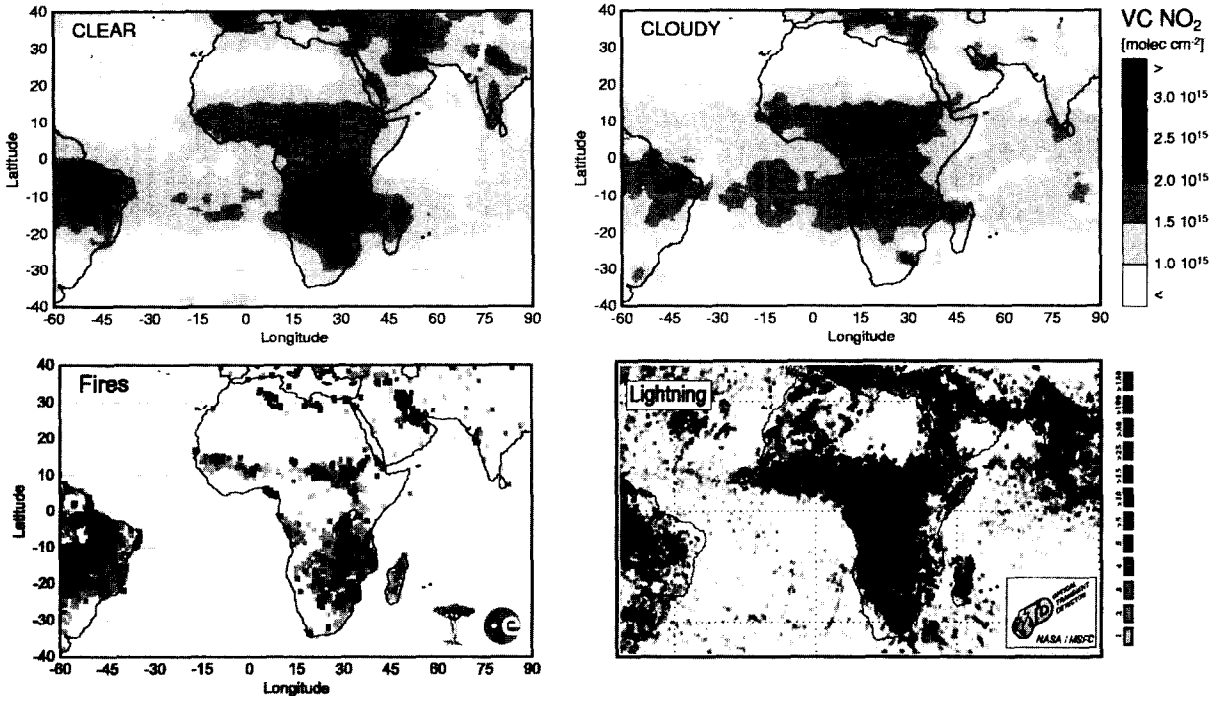

Fig. 8. GOME tropospheric NO_2 columns, ATSR fire counts and OTD lightning above Africa in fall 1997. In the upper left panel, cloud free pixels have been selected (ICFA < 0.1), in the upper right panel only cloudy pixels (ICFA > 0.3) have been used. In the clear sky data, pronounced NO_2 emissions from biomass burning in southern Africa and Brazil can be identified along with anthropogenic emissions in Europe, Arabia and South Africa. In the cloudy data, a NO_2 background over the African continent and elevated values over both the Atlantic and the Pacific are visible, indicating the presence of substantial amounts of NO_2 above the clouds.

et al. [1989]) measurements, implying that substantial amounts of NO_2 are produced from lightning. Perhaps most surprising, there is a plume of elevated NO_2 extending from Africa over the South Atlantic and also into the Indian Ocean. These plumes coincide with areas where enhanced tropospheric ozone has been observed in earlier years (*Fishman et al.* [1996]), indicating that NO_2 from biomass burning and lightning is transported over large distances and can play an important role in the formation of tropospheric ozone.

Information on the vertical distribution of the observed tropospheric NO_2 can be obtained by comparing the clear sky data with measurements taken over clouds. As discussed in the previous sections, NO_2 in the boundary layer is effectively blocked from view if clouds are present. Accordingly, the cloudy data show only small enhancements in regions of anthropogenic emissions or biomass burning. However, the background values over Africa and the enhancement over the Atlantic and the Indian Ocean are not only still present but often enhanced over the clear sky values. This implies, that substantial NO_2 is present above the clouds in the free troposphere and can contribute to *in-situ* production of ozone in remote regions.

The quantification of the NO_x above the clouds is complicated by the change in airmass factor to be used in the GOME measurements (see *Hild et al.* [2001]), the change in the partitioning between NO and NO_2 resulting from the increase of j_{NO_2} above clouds and the fact, that GOME always samples the atmosphere at the same time late in the morning. However, the results already show, that 1) NO_2 is present in the free troposphere both in regions with and without biomass burning implying an important contribution from lightning and 2) that NO_2 is transported over the South Atlantic and the Indian Ocean, enabling in situ production of ozone in these regions.

SUMMARY

In this study, GOME measurements have been analysed for tropospheric NO_2 using the DOAS method. The tropospheric excess column has been derived from the total columns using the Pacific sector as a clean air reference. The error budget has been discussed in detail, and uncertainties in the tropospheric light path and cloud cover have been identified as the largest contributions to the overall error. The derived tropospheric columns have a total uncertainty of up to a factor of 2 from the uncertainty in enhancement factor and $1 \cdot 10^{15}$ molec/cm^2 from other error sources. Most errors tend to lead to an underestimation of the tropospheric column. Accordingly, the GOME results should be interpreted as lower limits for the tropospheric NO_2 loading.

A case study of tropospheric NO_2 above Africa in fall 1997 revealed signature of anthropogenic NO_2 sources as well as NO_2 from biomass burning and strong indication for contributions from lightning. The latter is supported by comparison of clear and cloudy pixels, that show large differences for regions where NO_2 sources are located in the boundary layer but small changes for the background values, implying that this NO_2 must be located in the free troposphere. The analysis also provides evidence for long range transport of NO_2 over the Southern Atlantic and the Indian Ocean, with implications for the mechanism of ozone production in these regions.

ACKNOWLEDGMENTS

Helpful discussions with S. Solomon, F. Wittrock, T. Wagner and J. Trentmann are gratefully acknowledged. Lightning data from the Optical Transient Detector have been provided by NASA through the internet site `http://thunder.nsstc.nasa.gov/data/otdbrowse.html`. Parts of this work have been funded by the University of Bremen, the European Union under contract EVK2-CT-1999-00011 and the German Space Agency (DARA).

REFERENCES

Burrows, J. P., et al., The Global Ozone Monitoring Experiment (GOME): Mission Concept and First Scientific Results, *J. Atmos. Sci.*, **56**, 151–175, 1999a.

Burrows, J. P., A. Dehn, B. Deters, S. Himmelmann, A. Richter, S. Voigt, and J. Orphal, Atmospheric remote-sensing reference data from GOME: Part 1. Temperature-dependent absorption cross-sections of NO_2 in the 231–794 nm range, *J. Quant. Spectrosc. Rad. Transfer*, **60**, 1025–1031, 1998.

Burrows, J. P., A. Richter, A. Dehn, B. Deters, S. Himmelmann, S. Voigt, and J. Orphal, Atmospheric remote-sensing reference data from GOME: Part 2. Temperature-dependent absorption cross-sections of O_3 in the 231–794 nm range, *J. Quant. Spectrosc. Rad. Transfer*, **61**, 509–517, 1999b.

Chance, K., Analysis of BrO measurements from the Global Ozone Monitoring Experiment, *Geophys. Res. Lett.*, **25**, 3335–3338, 1998.

Chance, K., P. I. Palmer, R. J. D. Spurr, R. V. Martin, T. P. Kurosu, and D. J. Jacob, Satellite observations of formaldehyde over North America from GOME, *Geophys. Res. Lett.*, **27**, 3461–3464, 2001.

Christian, H. J., R. J. Blakeslee, and S. J. Goodman, The Detection of Lightning from Geostationary Orbit, *J. Geophys. Res.*, **94**, 13329–13337, 1989.

Eisinger, M., and J. P. Burrows, Tropospheric Sulfur Dioxide observed by the ERS-2 GOME instrument, *Geophys. Res. Lett.*, **25**, 4177–4180, 1998.

European Space Agency ESA/ESRIN via Galileo Galilei CP 64 00044 Frascati Italy, I., ATSR World Fire Atlas, `http://shark1.esrin.esa.it/FIRE/AF/ATSR`, 2000.

Feister, U., and R. Grewe, Spectral albedo measurements in the UV and visible region over different types of surfaces, *Photochem.Photobiol.*, **62**, 736–744, 1995.

Fishman, J., V. G. Brackett, E. V. Browell, and W. B. Grant, Tropospheric ozone derived from TOMS/SBUV measurements during TRACE A, *J. Geophys. Res.*, **101**, 24069–24082, 1996.

GOME, G. O. M. E., Users manual, 1995.

Greenblatt, G. D., J. J. Orlando, J. B. Burkholder, and A. R. Ravishankara, Absorption measurements of oxygen between 330 and 1140 nm, *J. Geophys. Res.*, **95**, 18577–18582, 1990.

Herman, J. R., and E. A. Celarier, Earth surface reflectivity climatology at 340-380 nm from TOMS data, *J. Geophys. Res.*, **102**, 28003–28012, 1997.

Hild, L., A. Richter, V. Rozanov, and J. P. Burrows, Air mass calculations for gome measurements of lightning-produced NO_2, this issue.

Koelemeijer, R. B. A., and P. Stammes, Validation of Global Ozone Monitoring Experiment cloud fractions relevant for accurate ozone column retrieval, *J. Geophys. Res.*, **104**, 18801–18814, 1999.

Kurosu, T., V. V. Rozanov, and J. P. Burrows, Parametrization schemes for terrestrial water clouds in the radiative transfer model GOMETRAN, *J. Geophys. Res.*, **102**, 21809–21823, 1997.

Ladstätter-Weißenmayer, A., J. P. Burrows, P. Crutzen, and A. Richter, GOME: Biomass burning and its influence on the troposphere, in *European Symposium on Atmospheric Measurements from Space, ESA WPP-161*, vol. 1, pp. 369–374, 1999.

Lamarque, J. F., G. P. Brasseur, P. G. Hess, and J. F. Müller, Three-dimensional study of the relative contributions of the different nitrogen sources in the troposphere, *J. Geophys. Res.*, **101**, 22955–22968, 1996.

Leue, C., M. Wenig, T. Wagner, O. Klimm, U. Platt, and B. Jähne, Quantitative analysis of NO_x emissions from GOME satellite image sequences, *J. Geophys. Res., in press*.

Li, Z., and L. Garand, Estimation of surface albedo from space: a parametrization for global applications, *J. Geophys. Res.*, **99**, 8335–8350, 1994.

Richter, A., Absorptionsspektroskopische Messungen stratosphärischer Spurengase über Bremen, 53°N, Ph.D. thesis, University of Bremen, 1997.

Richter, A., F. Wittrock, M. Eisinger, and J. P. Burrows, GOME observations of tropospheric BrO in Northern Hemispheric spring and summer 1997, *Geophys. Res. Lett.*, **25**, 2683–2686, 1998.

Rothman, L. S., et al., The HITRAN molecular database editions 1991 and 1992, *J. Quant. Spectrosc. Radiat. Transfer*, **48**, 469–507, 1992.

Rozanov, V., D. Diebel, R. J. D. Spurr, and J. P. Burrows, GOMETRAN: A radiative transfer model for the satellite project GOME - the plane parallel version, *J. Geophys. Res.*, **102**, 16683–16696, 1997.

Schultz, M. G., et al., On the origin of tropospheric ozone and NO_x over the tropical South Pacific, *J. Geophys. Res.*, **104**, 5829–5843, 1999.

Solomon, S., A. L. Schmeltekopf, and W. R. Sanders, On the interpretation of zenith sky absorption measurements, *J. Geophys. Res.*, **92**, 8311–8319, 1987.

Thomas, W., E. Hegels, S. Slijkhuis, R. Spurr, and K. Chance, Detection of biomass burning combustion products in Southeast Asia from backscatter data taken by the GOME spectrometer, *Geophys. Res. Lett.*, **25**, 1317–1320, 1998.

Thompson, A. M., et al., Ozone over southern Africa during SAFARI-92/TRACE A, *J. Geophys. Res.*, **101**, 23793–23807, 1996.

Velders, G. J. M., C. Granier, R. W. Portmann, K. Pfeilsticker, M. Wenig, T. Wagner, U. Platt, A. Richter, and J. P. Burrows, Global tropospheric NO_2 column distributions: Comparing 3-D model calculations with GOME measurements, *J. Geophys. Res., in press*.

Vountas, M., V. V. Rozanov, and J. P. Burrows, Ring effect: Impact of rotational Raman scattering on radiative transfer in earth's atmosphere, *J. Quant. Spectrosc. Radiat. Transfer*, **60**, 943–961, 1998.

Wagner, T., and U. Platt, Satellite mapping of enhanced BrO concentrations in the troposphere, *Nature*, **395**, 486–490, 1998.